Efficient white organic light-emitting diodes comprising an ultrathin iridium complex sub-monolayer



2007 J. Phys. D: Appl. Phys. 40 2783

(http://iopscience.iop.org/0022-3727/40/9/017)

IOP Publishing Journal of Physics D: Applied Physics
J. Phys. D: Appl. Phys. **40** (2007) 2783–2786 doi:10.1088/0022-3727/40/9/017

# Efficient white organic light-emitting diodes comprising an ultrathin iridium complex sub-monolayer

**Zisheng Su[1,2], Wenlian Li[1,3], Maoliang Xu[1], Tianle Li[1,2], Dan Wang[1,2], Wenming Su[1,2], Jinghua Niu[1,2], Hong He[1], Jianzhuo Zhu[1,2] and Bei Chu[1]**

[1] Key Laboratory of Excited State Processes, Changchun Institute of Optics, Fine Mechanics and Physics, Chinese Academy of Sciences, Changchun 130033, People's Republic of China
[2] Graduate School of Chinese Academy of Sciences, Beijing 100039, People's Republic of China

E-mail: wllioel@yahoo.com.cn

Received 31 December 2006, in final form 15 March 2007
Published 19 April 2007
Online at stacks.iop.org/JPhysD/40/2783

**Abstract**
Efficient white organic light-emitting diodes (WOLEDs) in which the blue and red emissions come from bis[(4,6-diflourophenyl)pyridinato-N,$C^{2'}$] (picolinato)iridium(III) and bis[2-(2′-benzothienyl)pyridinato-N,$C^{3'}$] (acetylacetonato)iridium(III) doped 4,4′-N,N′-dicarbazole-biphenyl (CBP) layers while the green emission comes from an ultrathin non-doped *fac*-tris[2,5-di(4-methoxyphenyl) pyridinato-C,N]iridium(III) [Ir(dmoppy)$_3$] sub-monolayer are demonstrated. The electroluminescent spectra of the devices can be fine tuned by the Ir(dmoppy)$_3$ thickness. The optimized device with 0.25 nm Ir(dmoppy)$_3$ shows a maximum current efficiency, power efficiency and luminance of 10.8 cd A$^{-1}$, 4.5 lm W$^{-1}$ and 12560 cd m$^{-2}$, respectively. Atomic force microscopy images reveal that the ultrathin non-doped layer is discontinuous. When sandwiched between the CBP and bathocuproine (BCP) layers, it forms a doping profile similar to the situation when the Ir(dmoppy)$_3$ is doped into CBP and BCP simultaneously.

## 1. Introduction

White organic light-emitting diodes (WOLEDs) have drawn considerable attention due to their potential applications as full colour displays, backlights for liquid-crystal displays and even next generation paper-thin lighting sources [1–10]. White light emission in organic light-emitting diodes (OLEDs) can be obtained by mixing two complementary colours or three primary colours. For lighting and full colour displays, a combination of the three primary colours is required to fully span the entire visible spectrum. There are many methods to achieve white light emission, including single layer polymer blends [11, 12], exciplexes [13, 14], hybrid organic/inorganic structures [15, 16] or multilayer structures [17–20]. Among these strategies, multilayer technology based on phosphorescent materials which have the potential for achieving 100% internal quantum efficiency [21] stands out as the most effective mechanism for WOLEDs. Recently, the non-doped strategy has been adopted for WOLEDs to simplify the fabrication process. There are many reports on fluorescent WOLEDs based on this non-doped strategy [22–25]; however, there are few reports on the phosphorescent WOLEDs based on this strategy.

In this communication, we report on WOLEDs in which the blue and red emissions come from bis[(4,6-diflourophenyl) pyridinato-N,$C^{2'}$](picolinato)iridium(III) (FIrpic) and bis[2-(2′-benzothienyl) pyridinato-N, $C^{3'}$] (acetylacetonato)iridium (III)[btp$_2$Ir(acac)] doped 4,4′-N,N′-dicarbazole-biphenyl (CBP) layers, respectively, and the green emission comes from an ultrathin non-doped *fac*-tris[2,5-di(4-methoxyphenyl)pyridinato-C,N]iridium(III) [Ir(dmoppy)$_3$] layer. Figure 1 shows

[3] Author to whom any correspondence should be addressed.

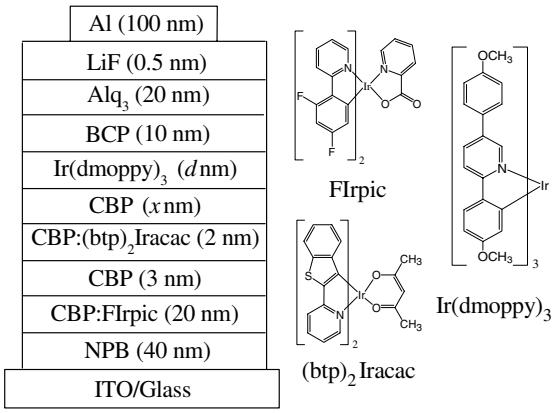


**Figure 1.** Device structure of the WOLEDs and the chemical structures of the materials used.

the chemical structures of the phosphorescent materials used here, and these three phosphorescent materials were synthesized in our laboratories. The green emitter, $Ir(dmoppy)_3$, was demonstrated as an excellent emitter whose performances are superior to the traditional one, *fac*-tri(phenylpyridine)iridium(III) [$Ir(ppy)_3$] [26]. Incorporating a methoxyl and a 4-methoxyphenyl onto the 4- and 5-positions of the pyridyl ring not only brings a 20 nm red shift of the spectrum, which is essential for the WOLEDs to fully span the entire visible spectrum compared with that of $Ir(ppy)_3$, but also prevents the intermolecular aggregation between the $Ir(dmoppy)_3$ molecules due to the extended spatial block effect.

## 2. Experimental

The WOLEDs have the structures of indium tin oxide (ITO)/NPB (40 nm)/CBP: FIrpic (8 wt%, 20 nm)/CBP (3 nm)/CBP:$btp_2Ir(acac)$ (4 wt%, 2 nm)/CBP (*x* nm)/$Ir(dmoppy)_3$ (*d* nm)/BCP (10 nm)/$Alq_3$ (20 nm)/LiF (0.5 nm)/Al (100 nm), as shown in figure 1, where, N,N′-diphenyl-N,N′-bis(1-naphthyl)-(1,1′-benzidine)-4,4′-diamine (NPB), bathocuproine (BCP) and tris(8-hydroxyquinoline)aluminium ($Alq_3$) act as the hole-transporting layer, exciton-blocking layer and electron-transporting layer, respectively. Two non-doped CBP layers were used as spacers to separate the three emission regions and prevent the energy transfer from the higher energy emitters to the lower one. The thickness of the spacer inserted in the CBP : FIrpic/CBP : $btp_2Ir(acac)$ interface was fixed at 3 nm, while the one in the CBP : $btp_2Ir(acac)$/$Ir(dmoppy)_3$ interface was changed. Two series devices, one with a different $Ir(dmoppy)_3$ thickness and the other with a different CBP spacer thickness, were fabricated. Organic layers were deposited onto a pre-cleaned ITO glass substrate (25 Ω/square) by thermal evaporation in a vacuum chamber at $3 \times 10^{-4}$ Pa, followed by a LiF buffer layer and an Al cathode in the same vacuum run. Deposition rates and thicknesses of the layers were monitored *in situ* using an oscillating quartz monitor. The evaporating rates were kept at 0.2–0.5 Å $s^{-1}$ for $Ir(dmoppy)_3$ layer, 0.5–1 Å $^{-1}$s for other organic layers and LiF layer and 10 Å $s^{-1}$ for the Al cathode, respectively. Due to the island nature of the ultrathin $Ir(dmoppy)_3$ layers, the thicknesses of these

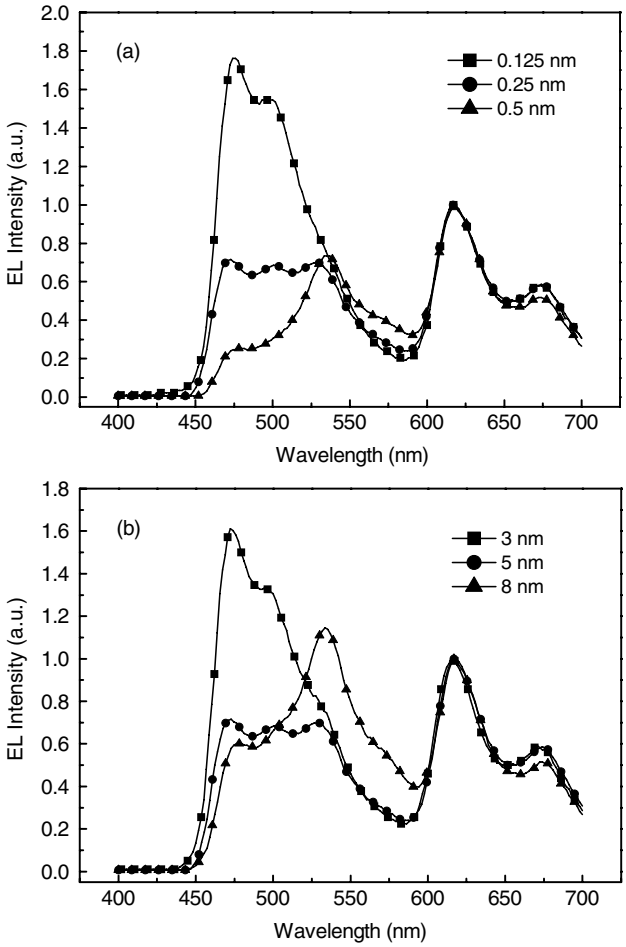


**Figure 2.** (*a*) Effect of the $Ir(dmoppy)_3$ thickness on the EL spectra at 10 V. (*b*) Effect of the CBP thickness on the EL spectra at 10 V.

layers only represent the densities of the islands. Electroluminescent (EL) spectra and CIE coordinates of these devices were measured by a Hitachi MPF-4 fluorescence spectrophotometer. The luminance–current–voltage (*L–I–V*) characteristics were measured with a 3645 dc power supply combined with a spot photometer and were recorded simultaneously with measurements. The morphologies of 0.5 nm $Ir(dmoppy)_3$ and 30 nm CBP coated silicon wafers were examined using a Nanoscope Dimension$^{TM}$ 3100 atomic force microscope (AFM); meanwhile, the morphology of the silicon wafer was also examined for reference. All the measurements were carried out at room temperature under ambient conditions.

## 3. Results and discussions

Figure 2(*a*) shows the normalized EL spectra of the devices with different $Ir(dmoppy)_3$ thicknesses when the CBP layer was fixed at 5 nm at an applied bias of 10 V. The blue, green and red emissions of 472 nm with the shoulder at 500 nm, 531 nm and 618 nm with the shoulder at 670 nm come from FIrpic, $Ir(dmoppy)_3$ and $btp_2Ir(acac)$, respectively. The emission of FIrpic decreases relative to that of $btp_2Ir(acac)$ with an increased $Ir(dmoppy)_3$ layer thickness; correspondingly, the CIE coordinates shift from (0.31,0.30) to (0.45,0.46). Under the electrical field, excitons are predominantly formed in the

**Table 1.** Devices' performances.

| $Ir(dmoppy)_3$ thickness (nm) | CBP thickness (nm) | Max efficiency ($cd\,A^{-1}$) | Max $\eta_p$ ($lm\,W^{-1}$) | Max luminance ($cd\,m^{-2}$) | CIE coordinates at 10 V |
|---|---|---|---|---|---|
| 0.12 | 5 | 8.1 | 4.2 | 9480 | (0.30,0.31) |
| 0.25 | 3 | 6.4 | 3.3 | 11540 | (0.32,0.32) |
| 0.25 | 5 | 10.8 | 4.5 | 12560 | (0.39,0.38) |
| 0.25 | 8 | 11.9 | 5.6 | 14100 | (0.39,0.45) |
| 0.50 | 5 | 12.1 | 5.4 | 15640 | (0.45,0.46) |

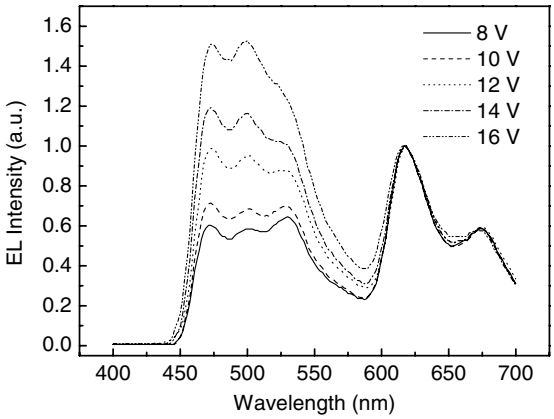


**Figure 3.** EL spectra of the optimized WOLED under different biases.

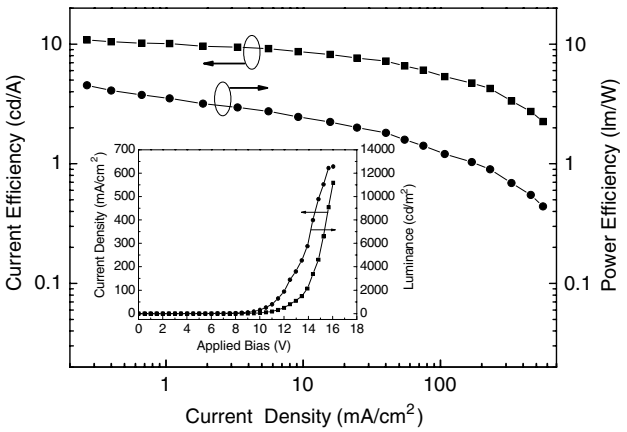


**Figure 4.** Current efficiency and power efficiency versus current density of the optimized WOLED. Inset: Current density–voltage–luminance characteristics of the optimized device.

region of the emitting layer adjacent to the BCP exciton-blocking layer. Excitons can be formed on CBP molecules as well as on the emitters directly after they trap the holes and electrons. The excitons on CBP can diffuse to the layer far from the excitons formation layer, i.e. the FIrpic doped CBP layer, due to the triplet excitons typically having long diffuse lengths [27]. Increased $Ir(dmoppy)_3$ layer thickness would increase the number of excitons formation in $Ir(dmoppy)_3$ and the energy transfer from CBP to $Ir(dmoppy)_3$, and hence reduce the excitons diffusion to the FIrpic. With the increased emission of $Ir(dmoppy)_3$, the efficiency of the device increases from 8.1 to 12.1 $cd\,A^{-1}$ when the $Ir(dmoppy)_3$ thickness increases from 0.12 to 0.50 nm. Figure 2(*b*) shows the normalized EL spectra of the devices with different CBP spacer layer thicknesses when the $Ir(dmoppy)_3$ thickness was fixed at 0.25 nm at an applied bias of 10 V. It can be found that the $Ir(dmoppy)_3$ emission increased with the CBP layer thickness due to the decreased energy transfer from $Ir(dmoppy)_3$ to $btp_2Ir(acac)$; correspondingly, the CIE coordinates of the devices changes from (0.32,0.32) to (0.39,0.45). Similarly, the increased $Ir(dmoppy)_3$ emission also leads to the increased device efficiency. Table 1 summarizes the performances of the devices with different $Ir(dmoppy)_3$ and/or CBP thicknesses.

Figure 3 shows normalized EL spectra of the optimized device with 0.25 nm $Ir(dmoppy)_3$ and 5 nm CBP layers at different applied biases. As the applied bias of the device increases, the emission of FIrpic increases due to the saturated emission of $Ir(dmoppy)_3$ and $btp_2Ir(acac)$ and the changed recombination zone at a higher current density. The CIE coordinates of the device at 8 V, 10 V, 12 V, 14 V and 16 V are (0.41, 0.39), (0.39, 0.38), (0.36, 0.37), (0.33, 0.36) and (0.32, 0.36), respectively, and all these coordinates are in the white region.

Figure 4 plots the current efficiency and power efficiency as a function of current density of the optimized device. The maximum current efficiency and power efficiency of 10.8 $cd\,A^{-1}$ and 4.5 $lm\,W^{-1}$ are achieved at a current density of 0.26 $mA\,cm^{-2}$ and then gradually decrease with the increased current density due to triplet–triplet annihilation [28]. The lower efficiencies of the device compared with the other reported phosphorescent WOLEDs may be due to the lower purities of the phosphorescent materials. The device has a turn on voltage of about 4.2 V and a maximum luminance of 12560 $cd\,m^{-2}$ at an applied bias of 16 V, as shown in the inset of figure 4.

To further understand the effect of the ultrathin non-doped $Ir(dmoppy)_3$ layer inserted between the CBP and the BCP layers, the surface state of the ultrathin non-doped $Ir(dmoppy)_3$ layer was investigated by atomic force microscopy (AFM). Figure 5 shows the morphologies of the bare silicon wafer, 0.5 nm $Ir(dmoppy)_3$ and 30 nm CBP coated silicon wafers. It can be noted that the 0.5 nm $Ir(dmoppy)_3$ film is discontinuous and there are some islands separated by gaps, while the morphology of CBP is rough. When the ultrathin $Ir(dmoppy)_3$ sub-monolayer is deposited onto the rough CBP layer followed by a BCP layer, then from the structural viewpoint, it is similar to the dope-type device in which the $Ir(dmoppy)_3$ is doped into CBP and BCP simultaneously. Different from the conventional doped devices which have a doped layer extended up to several nanometres, this type of devices only have an ultrathin doped layer due to the $Ir(dmoppy)_3$ molecules distributed in two dimensions.

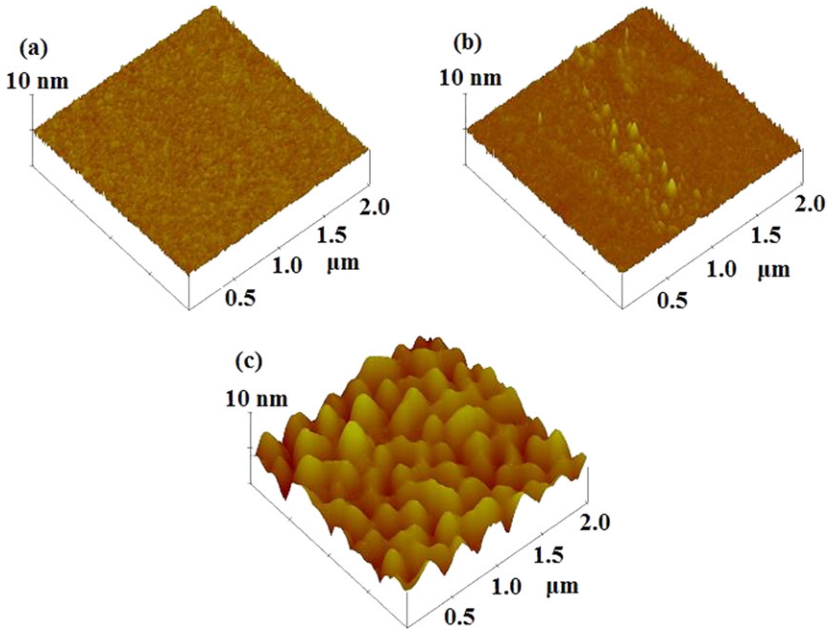


**Figure 5.** AFM images of silicon wafer (*a*), 0.5 nm Ir(dmoppy)$_3$ (*b*) and 30 nm CBP (*c*) coated silicon wafers. (This figure is in colour only in the electronic version)

## 4. Summary

In summary, efficient WOLEDs comprising an ultrathin non-doped Ir(dmoppy)$_3$ layer were presented. The optimized device shows a maximum current efficiency, power efficiency and luminance of 10.8 cd A$^{-1}$, 4.5 lm W$^{-1}$ and 12560 cd m$^{-2}$, respectively. All the CIE coordinates of the devices are in the white region from 8 to 16 V. The AFM images reveal that the ultrathin non-doped Ir(dmoppy)$_3$ layer is discontinuous with some islands and formed a doping profile when sandwiched between the CBP and BCP layers. Our finding has potential use in simplifying the architecture and fabrication process of the OLEDs and hence cutting down the cost.

## Acknowledgment

The authors acknowledge the National Natural Science Foundation of China (Grant No 90201012) for support of this research.

## References

[1] Kido J, Shionoya H and Nagai K 1995 *Appl. Phys. Lett.* **67** 2281
[2] Sun Y, Giebink N C, Kanno H, Ma B, Thompson M E and Forrest S R 2006 *Nature* **440** 908
[3] Cheon K O and Shinar J 2002 *Appl. Phys. Lett.* **81** 1738
[4] Tokito S, Lijima T, Tsuzuki T and Sato F 2003 *Appl. Phys. Lett.* **83** 2459
[5] Qin D and Tao Y 2005 *Appl. Phys. Lett.* **86** 113507
[6] Li J Y, Liu D, Ma C, Lengyel O, Lee C S, Tung C H and Lee S 2004 *Adv. Mater.* **16** 1538
[7] Niu J H, Li W L, Wei H Z, Li M T, Su W M, Xin Q, Zhang Z Q and Hu Z Z 2005 *J. Phys. D: Appl. Phys.* **38** 1136
[8] Shih P I, Shu C F, Tung Y L and Chi Y 2006 *Appl. Phys. Lett.* **88** 251110
[9] Lei G, Wang L and Qiu Y 2006 *Appl. Phys. Lett.* **88** 103508
[10] Yu X M, Kwok H S, Wong W Y and Zhou G J 2006 *Chem. Mater.* **18** 5097
[11] Tasch S, List E J W, Ekström O, Graupner W, Leising G, Schlichting P, Rohr U, Geerts Y, Scherf U and Müllen K 1997 *Appl. Phys. Lett.* **71** 2883
[12] Niu X, Ma L, Yao B, Ding J, Tu G, Xie Z and Wang L 2006 *Appl. Phys. Lett.* **89** 213508
[13] Hide F, Kozodoy P, Denbaars S P and Heeger A J 1997 *Appl. Phys. Lett.* **70** 2664
[14] Li M, Li W, Chen L, Kong Z, Chu B. Li B, Hu Z and Zhang Z 2006 *Appl. Phys. Lett.* **88** 091108
[15] Duggal A R, Shlang J J, Heller C M and Foust D F 2002 *Appl. Phys. Lett.* **80** 3470
[16] Xuan Y, Pan D, Zhao N, Ji X and Ma D 2006 *Nanotechnology* **17** 4966
[17] D'Andrade B W, Brooks J, Thompson M E and Forrest S R 2002 *Adv. Mater.* **14** 147
[18] Cheng G, Zhang Y, Zhao Y and Liu S 2006 *Appl. Phys. Lett.* **88** 083512
[19] Xie W F, Chew S L, Lee C S, Lee S T, Wang P F and Kwong H L 2006 *J. Appl. Phys.* **100** 096114
[20] Kanno H, Sun Y and Forrest S R 2006 *Appl. Phys. Lett.* **89** 143516
[21] Adachi C, Baldo M A, Thompson M E and Forrest S R 2001 *J. Appl. Phys.* **90** 5048
[22] Tsuji T, Naka S, Okada H and Onnagawa H 2002 *Appl. Phys. Lett.* **81** 3329
[23] Cheng G, Zhao Y, Zhang Y, Liu S, He F, Zhang H and Ma Y 2004 *Appl. Phys. Lett.* **84** 4457
[24] Yang H, Zhao Y, Xie W, Shi Y, Hu W Meng Y, Hou J and Liu S 2006 *Semicond. Sci. Technol.* **21** 1447
[25] Xie W, Wu Z, Liu S and Lee S T 2003 *J. Phys. D: Appl. Phys.* **36** 2331
[26] Xu M L, Li T L, Li W L, Hong Z R, An Z W and Zhou Q 2006 *Thin Solid Films* **497** 239
[27] Baldo M A, O'Brien D F, Thompson M E and Forrest S R 1999 *Phys. Rev.* B **60** 14422
[28] Baldo M A, Adachi C and Forrest S R 2000 *Phys. Rev.* B **62** 10967